Post-polymerization modification of phosphorus containing conjugated copolymers

Hongda Cao[a], Nicole Bauer[b], Sheng Bi[c,1], Dawen Li[c], Wei You[b], Paul A. Rupar[a,*]

[a] Department of Chemistry and Biochemistry, University of Alabama, Tuscaloosa, AL 35487, United States
[b] Department of Chemistry, University of North Carolina at Chapel Hill, Chapel Hill, NC 27599, United States
[c] Department of Electrical and Computer Engineering, Center for Materials for Information Technology, The University of Alabama, Tuscaloosa, AL 35487, United States

ABSTRACT

A new phosphafluorene (PF) based monomer, featuring a phosphine oxide substituted with a dodecyl chain, was synthesized. PF was copolymerized with benzodithiophene (BDTT) to form the copolymer PPF-BDTT which has a donor (BDTT)–acceptor (PF) structure. For the first time, direct post-polymerization modifications were performed on the phosphorus center of phosphafluorene-containing conjugated polymers. With Lawesson's Reagent, PPF-BDTT was transformed from a phosphine oxide to a phosphine sulfide. Reduction of the phosphine oxide of PPF-BDTT with $HSiCl_3$, followed by reaction with $AuCl \cdot SMe_2$, produced PPF-BDTT-Au, which contains AuCl coordinated to the phosphafluorene moiety. PPF-BDTT, PPF-BDTT-S, and PPF-BDTT-Au were characterized optically and electrochemically and the results compared to related BDTT containing copolymers. PPF-BDTT and its derivatives were found to have high LUMO and HOMO levels and larger bandgaps compared to common donor-acceptor copolymers. Organic solar cells were fabricated from PPF-BDTT, PPF-BDTT-S, and PPF-BDTT-Au, although the performances of these devices were poor with power conversion efficiencies ranging from 0.13% to 0.60%.

1. Introduction

Conjugated polymers (CPs) have been researched intensively for their applications in photovoltaic cells (PVCs) [1–6], organic field effect transistors (OFETs) [7–10], organic light-emitting diodes (OLEDs) [11,12], and sensors [13–15]. Due to its ease of synthesis, fluorene is one of the most commonly used moieties in CPs. However, fluorene based CPs tend to have large bandgaps and high HOMO energy levels which limits their use in situations where lower lying HOMOs and narrow bandgaps are desirable [16–18]. A common strategy to modify the properties of conjugated materials is to embed inorganic elements into the conjugated systems [19–22]. Using fluorene as an example, this can be accomplished by the replacement of the 9-carbon on fluorene. Many inorganic-element containing fluorenes and their resulting polymers (Fig. 1) have been developed, including silafluorene [23,24], carbazole [25,26], and germafluorene [27–29]. These have been used as effective electron donors in high-performance PVCs [25,30], OFETs [24], and as in-vivo bio-imaging agents [23]. Borafluorene possesses strong electron-withdrawing properties [20,31–34], and its homopolymer showed reversible fluorescence sensing of NH_3 vapor [35]. Gallafluorene was reported by Chujo and coworkers and its

corresponding polymers exhibit controllable emission color by changing the co-monomer units [36,37].

Phosphorus containing conjugated systems are particularly interesting due to their high versatility and tunability [38–41]. In addition to the possibility of two different oxidation states (phosphorus(III) and phosphorus(V)), the lone pair of electrons of phosphorus(III) are accessible for functionalization with transition metals and other Lewis acids (Fig. 2) [42–44]. The Réau group has reported on small molecule phospholes, including phosphine, phosphine sulfide, and gold(I) coordinated derivatives, and their resulting use in OLEDs [45,46]. However, to our best knowledge, the modifications of the phosphorus center have mostly been performed in conjugated small molecules, and only few in conjugated polymers reported [47,48]. Recently, Park and Kim designed a series of dithienophosphole oxide (DTP) containing polymers and showed these to have power conversion efficiencies (PCEs) greater than 6.5% when incorporated into solar cells [49,50]. These high efficiencies were hypothesized to occur because of improved charge separation due to the large dipole moment of the phosphole oxide present in these polymers.

Phosphafluorene (PF), the phosphorus substituted fluorene, has received less attention in the literature relative to other heterofluorenes
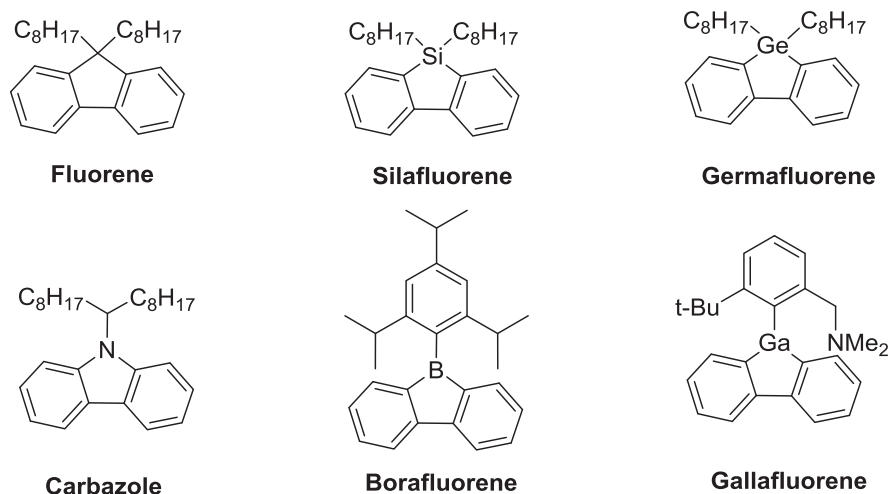

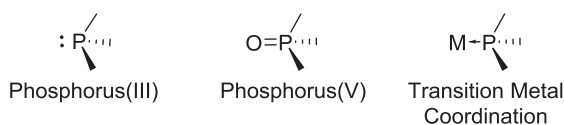**Fig. 1.** Fluorene and selected heterofluorenes.

Fig. 2. Tunable phosphorus center.

[51–54]. The synthesis of PF is most often achieved through lithiation of a biphenyl precursor [55], although alternative methods are known [56,57]. Reported applications of PF include an iridium complex that was used to create high external quantum efficiency OLEDs [53]. To the best of our knowledge, only two PF containing polymers are known, which were described by the Huang and Masato groups [51,58]. These polymers showed white or blue electrolumininescence with different substituents on the phosphorus centers [51,58].

Herein, we report on a series of novel phosphafluorene-based conjugated polymers. We examined a donor-acceptor (D-A) copolymer structure, with the phosphafluorene as an acceptor moiety and benzo-dithiophene (BDTT) as the donor moiety [59–62]. Direct post-polymerization modification of the phosphorus atoms within the polymers was performed, which demonstrated a new synthetic method to tune phosphorus containing conjugated polymers. The properties of the resulting polymers were measured, and their performance in polymeric organic solar cells was investigated.

2. Experiment

2.1. Instrument and materials

Gel permeation chromatography (GPC) was performed using a Malvern Viscotek VE 2001 Gel Permeation Chromatograph equipped with an automatic sampler, a pump, an injector, an inline degasser, a column oven (30 °C), and two in-series Malvern T6000M SEC columns. Reported molecular weights are versus a polystyrene standard. Detection was conducted by means of a photodiode array detector operating between 190 nm and 500 nm. Cyclic voltammograms (CVs) were acquired using a CHI760 potentiostat with a Pt wire quasi reference electrode and an Ag wire counter electrode. Scanning rates were kept at 0.1 V/s with a minimum 3 s quiet period before each scan. Ferrocene standards were added to the CV solution after measurements had been completed to avoid overlap of signals. Polymer CVs were measured by casting a film on the working electrode in a 0.1 M solution

of Bu_4NClO_4 in acetonitrile.

All manipulations were carried out under an anhydrous N_2 atmosphere using standard Schlenk line and glove box techniques. Solvents were dried by passing through an alumina column and then stored over 4 Å molecular sieves. 4,4′-dibromo-6,6′-diiodo-3,3′-dimethoxybiphenyl [55], 2,6-bis(trimethylstannyl)-4,8-bis(5-decylthiophen-2-yl)benzo [1,2-b:4,5b′]dithiophene (BDTT) [63] were synthesized according to known literature procedures. The synthesis of **1** was based on reports for similar dicholoro(alkyl)phosphanes [64]. All other reagents were purchased commercially and used without further purification.

2.2. Materials synthesis

2.2.1. Synthesis of 1-dodecylphosphonic dichloride (1)

1-dodecylphosphonic acid (2.5 g, 10 mmol) and DCM (30 mL) were combined. The mixture was heated to reflux for 30 mins, and a catalytic amount of DMF (2–3 drops) was added. Then excess oxalyl chloride (45 mmol, 4.0 mL) was added slowly into the mixture, and the resulting solution was refluxed for 12 h. The volatiles were removed by vacuum and a yellow oil was obtained with good purity (based on ^{31}P NMR) and was used directly in the next step. ^{1}H NMR (360 MHz, 298 K, CDCl$_3$): δ 0.86 (t, J = 7.2 Hz, 3H), 1.17–1.37 (m, 16H), 1.41–1.49 (m, 2H), 1.75–1.88 (m, 2H), 2.50–2.59 (m, 2H); ^{13}C NMR (125.7 MHz, 298 K, CDCl$_3$): δ 43.77, 42.70, 32.12, 29.96, 29.80, 29.72, 29.55, 29.44, 29.14, 29.13, 23.18, 23.11, 22.91, 14.34, 1.24; ^{31}P NMR (202.5 MHz, 298 K, CDCl$_3$): δ 51.23 (See Fig. S3–S5 in the Supporting Information for NMR spectra).

2.2.2. Synthesis of 2,7-dibromo-3,6-dimethoxy-9-dodecyl-9-phosphafluorene oxide (PF)

Butyl lithium (1.6 M in hexane, 2.0 mmol, 1.25 mL) was added dropwise to 4,4′-dibromo-6,6′-diiodo-3,3′-dimethoxybiphenyl (1.25 g, 2.0 mmol) dissolved in 50 mL of THF at −98 °C. The solution was stirred at −98 °C for 30 mins before 1-dodecylphosphonic dichloride (0.60 g, 2.1 mmol) in 10 mL of THF was added over 5 min. After 1 h, the solution was allowed to warm to room temperature and was then stirred for 15 h. The mixture was extracted by Et_2O three times. The organic layers were combined, dried with magnesium sulfate, and then removed under vacuum leaving an orange oil. The crude product was purified by chromatography on silica gel with hexane/ethyl acetate (1:1) to give the title compound as a yellow solid (0.34 g, 30% yield). ^{1}H NMR (360 MHz, 298 K, CDCl$_3$): δ 0.85 (t, J = 7.2 Hz, 3H), 1.15–1.34 (m, 18H), 1.40–1.49 (m, 2H), 2.02–2.04 (m, 2H), 4.04 (s, 6H), 7.15 (d,

$J = 3.6$ Hz, 2H), 7.91 (d, $J = 7.2$ Hz, 2H); ^{13}C NMR (125.7 MHz, 298 K, CDCl$_3$): δ 160.38, 160.36, 142.24, 142.08, 134.51, 134.42, 126.32, 125.50, 113.90, 113.79, 104.76, 104.67, 57.07, 32.37, 31.32, 31.20, 31.02, 30.45, 30.06, 29.98, 29.81, 29.79. 29.42, 23.14, 22.71, 22.68, 14.56; ^{31}P NMR (202.5 MHz, 298 K, CDCl$_3$): δ 40.56 (see Fig. S6–S8 in the Supporting Information for the NMR spectra); HRMS (EI, [M +], C$_{12}$H$_{20}$Br$_2$O$_2$Si$_2$): calcd, 584.0691; found, 584.0685. EA (%): Calculated for C$_{26}$H$_{35}$Br$_2$O$_3$P: C 53.26, H 6.02; found: C 53.49, H 6.17.

2.2.3. Synthesis of PPF-BDTT

The 2,6-Bis(trimethylstannyl)-4,8-bis(5-decylthiophen-2-yl)benzo [1,2-b:4,5b′]dithiophene monomer (0.1000 mmol, 101.7 mg), and PF (0.10 mmol, 58.6 mg), and Pd(PPh$_3$)$_4$ (0.0043 mmol, 5.0 mg,) were combined in 5 mL of dry toluene. The reaction mixture was stirred and heated to reflux for 24 h. Then the reaction mixture was cooled to room temperature, and the polymer was precipitated into 100 mL methanol, collected by filtration, and then purified via Soxhlet extraction with methanol and hexane, each for 12 h. Finally, the polymer was redissolved in chloroform and precipitated into methanol and the solid was collected and dried under vacuum overnight. The product was isolated as a dark red solid, 88 mg (79% yield). ^{31}P NMR (202.5 MHz, 298 K, CDCl$_3$): δ 42; GPC Data (vs PS standard): $M_n = 11.0$ kDa; Đ = 2.4; See Fig. S9 and S10 in the Supporting Information for NMR spectra.

2.2.4. Synthesis of PPF-BDTT-S

A dry toluene solution (20 mL) of PPF-BDTT (30 mg, 0.029 mmol) and Lawesson's Reagent (40 mg, 0.10 mmol) was heated to 110 °C overnight and stirred for 12 h. The reaction mixture was then cooled to room temperature and poured into methanol, resulting in the formation of an orange precipitate. The precipitate was collected and placed in a Soxhlet extractor. The precipitate was extracted with methanol and hexane, each for 12 h, and then dissolved in chloroform. Finally, the chloroform solution was precipitated in methanol and the solid was collected and dried under vacuum overnight to yield a brown-orange solid, 13.5 mg (45.0% yield). ^{31}P NMR (202.5 MHz, 298 K, CDCl$_3$): δ 45. See Fig. S11 and S12 in the Supporting Information for NMR spectra.

2.2.5. Synthesis of PPF-BDTT-Au

A toluene solution (15 mL) of PPF-BDTT (69 mg, 0.066 mmol); and trichlorosilane (0.10 mL, 1.0 mmol) was heated to 110 °C and stirred for 12 h. The reaction mixture was then cooled to room temperature and the solvents were removed by vacuum. The residue was then dissolved in dry DCM (20 mL) and chloro(dimethylsulfide)gold(I) (60 mg, 0.20 mmol) was added, and stirred for 3 h. The reaction mixture was poured into methanol, resulting in the formation of dark red precipitate. The precipitate was collected and placed in a Soxhlet extractor. The precipitate was extracted with methanol and hexane each for 12 h, and then dissolved in chloroform. Finally, the chloroform solution was precipitated in methanol, the solid was collected and dried under vacuum overnight to yield a red orange solid, 48.6 mg (59% yield). ^{31}P NMR (202.5 MHz, 298 K, CDCl$_3$): δ 20. See Figs. S13 and S14 in the Supporting Information for NMR spectra.

3. Results and discussion

3.1. Synthesis and characterization

The synthetic route of the phosphafluorene monomer (PF) is depicted in Scheme 1 and is based on a modified literature procedure [55]. The structure of PF is similar to previously reported fluorene monomers, except that the phosphorus is substituted with a dodecyl chain instead of the typically used phenyl moiety [51]. The dodecyl chain was chosen in an effort to increase the solubility of the resulting polymer.

Benzo[1,2-b:4,5-b′]dithiophene (BDTT) was selected as a co-monomer due to its planar structure, enhanced electron delocalization,

improved charge mobilities, and current popularity in CP research [65,66]. A Stille coupling between PF and benzodithiophene monomers was used to form the co-polymer PPF-BDTT. The ^{1}H NMR spectrum of PPF-BDTT (Fig. S9) was consistent with its proposed structure and ^{31}P NMR of the polymer (Fig. S10) showed a single broad peak at 42 ppm, which is characteristic of a phosphine oxide. Analysis by GPC revealed that PPF-BDTT had a modest molecular weight of $M_n = 11.0$ kDa vs. a polystyrene standard. Attempts to increase the polymer molecular weight through the use of different conditions were not successful likely because of poor solubility at higher molecular weights.

A significant advantage of including phosphorus within a conjugate system is the potential to modify and tune the phosphorus center. This can lead to significant changes in the electronic properties of the conjugated material and also impact solubility [43,67–69]. In this work, we looked at three different modifications to the phosphorus center: transformation from the phosphine oxide to the phosphine sulfide, reduction to phosphorus(III), and coordination of AuCl to the phosphorus (III) center.

Attempts to reduce the phosphorus center in PPF-BDTT with HSiCl$_3$ were successful, although the resulting polymer rapidly re-oxidized back to the phosphine oxide in open air. However, subsequent coordination of AuCl·SMe$_2$ to the reduced polymer formed PPF-BDTT-Au, which is stable towards atmospheric oxygen. Reaction of PPF-BDTT with Lawesson's Reagent produced the phosphine sulfide PPF-BDTT-S. Unsurprisingly, the ^{1}H NMR spectra of PPF-BDTT (Fig. S9), PPF-BDTT-S (Fig. S11), and PPF-BDTT-Au (Fig. S13) are nearly identical; fortunately, the ^{31}P NMR spectra are distinct and confirmed quantitative functionalization of the phosphorus center (Fig. 3). The ^{31}P NMR spectrum of PPF-BDTT-S (Fig. S12) showed a single signal at 45 ppm, which is consistent with a phosphine sulfide. The gold functionalized PPF-BDTT-Au exhibited a ^{31}P NMR (Fig. S14) chemical shift of 20 ppm, which is indicative of a phosphole gold chloride. All three polymers are modestly soluble in common organic solvents such as chloroform, dichlorobenzene, tetrachloroethane, and THF.
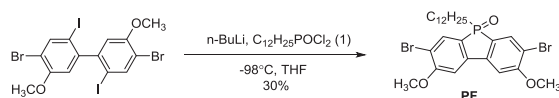
3.2. Optical properties

The UV–Vis absorption spectra of the polymers in dichloromethane (DCM) solution are shown in Fig. 4 and listed in Table 1. PPF-BDTT exhibited absorption bands centered at 425 nm in the UV which are attributed to the π-π* transitions and an absorption band at longer wavelength (centered at 465 nm), thought to originate from intra-molecular charge transfer. The absorption spectra of PPF-BDTT-S is very similar to that of PPF-BDTT. Conversely, PPF-BDTT-Au has a unique triple peak absorption pattern and redshift of ca. 65 nm. The emission spectra of PPF-BDTT and PPF-BDTT-S are similar, while PPF-BDTT-Au is distinctly redshifted (Fig. 4 and Table 1).

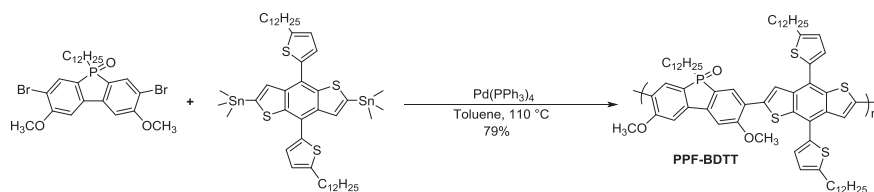### 3.3. Electrochemical properties

The electrochemical properties of polymer films were evaluated by cyclic voltammetry (Table 1 and Fig. S1). PPF-BDTT and PPF-BDTT-S had quasi-reversible oxidations and reductions. In the case of PPF-BDTT-Au, the oxidation was quasi-reversible, while the reduction was irreversible (Fig. S1). The HOMO and LUMO energy levels of these polymers were estimated from the CV oxidation and reduction onsets [70]. For PPF-BDTT, a LUMO of − 2.99 eV and HOMO of − 5.56 eV was determined. In comparison with PPF-BDTT, PPF-BDTT-S has a slightly lower LUMO level of − 3.03 eV. For PPF-BDTT-Au, it showed a higher lying HOMO level of − 5.23 eV and lower LUMO level of − 3.43 eV. Comparison of the band gaps ($E_{g,cv}$) show that PPF-BDTT-Au has by far the smallest $E_{g,cv}$ at 1.80 eV, whereas PPF-BDTT and PPF-BDTT-S are 2.56 eV and 2.43 eV, respectively.

Since there are many BDTT containing D-A copolymers in the literature and comparison to the PPF-BDTT copolymers described in this work can be made to provide insights into the influence of PF on
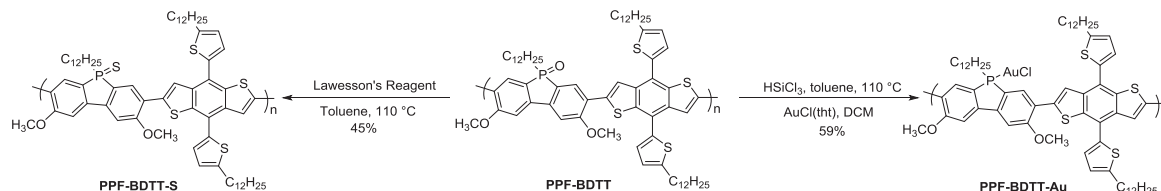
Monomer Synthesis

Polymerization via Stille Coupling Reaction

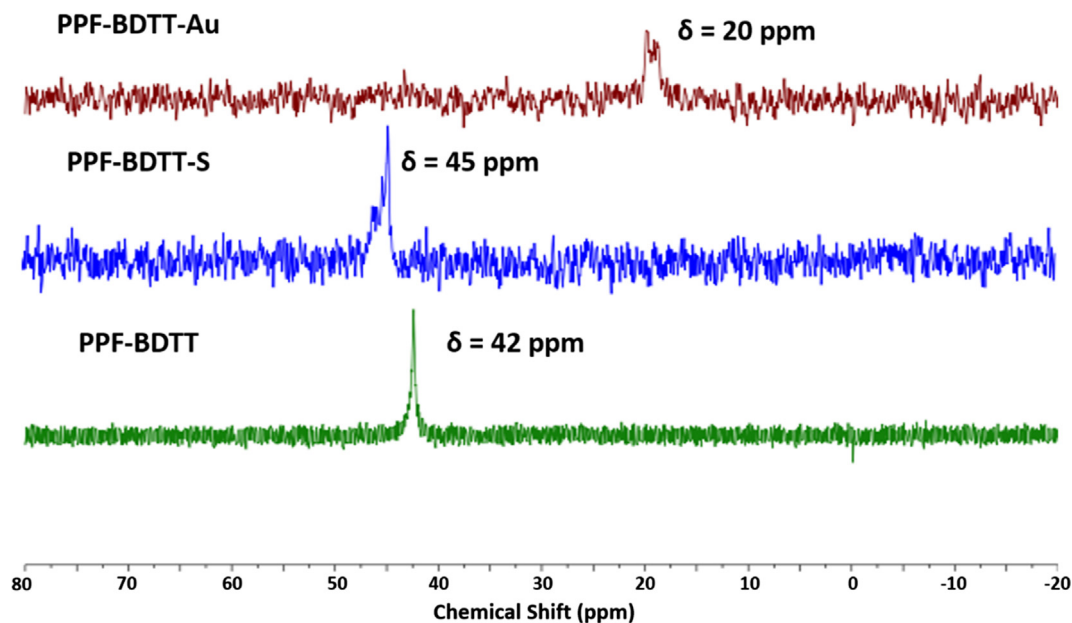**Post-polymerization Modification of PPF-BDTT**

Scheme 1. Synthesis of PPF-BDTT, PPF-BDTT-S, and PPF-BDTT-Au.

conjugated systems [49,63,70–72]. Fig. 5 depicts the HOMO and LUMO levels for a series of BDTT-containing copolymers, including the phosphaflourene containing copolymers reported in this work. Fig. 5 clearly shows that the LUMO and HOMO levels of PPF-BDTT, PPF-BDTT-S, and PPF-BDTT-Au are higher in energy than those of the other BDTT containing copolymers, suggesting that PF is significantly less electron withdrawing compared to other common acceptor moieties. We were especially surprised that the LUMO of PPF-BDTT is ca 0.97 eV higher than the phosphole containing copolymer PDTP-BDTT [49], in spite of the fact that the DTP group has two electron-rich thiophene moieties. We believe that the decreased accepting properties of PF likely arises due to the presence of the methoxy groups at the 3 and 6 positions, as well as the fact that the phosphorus center is substituted with an alkyl chain rather than the more electron withdrawing phenyl group found in DTP.

3.4. Device fabrication

To further explore the potential applications of these polymers, we fabricated organic solar cells using PPF-BDTT, PPF-BDTT-S, and PPF-BDTT-Au as electron donors with phenyl-C_{71}-butyric acid methyl ester ($PC_{71}BM$) as the electron acceptor. The performance details of these devices are summarized in Table S1, and the current density versus voltage (J–V) characteristics of representative devices are shown in Fig. S2. Among these three polymers devices, PPF-BDTT-S exhibited the best performance with an average power-conversion efficiency (PCE) of 0.60%, while PPF-BDTT-Au had a PCE of 0.26% and PPF-BDTT had a PCE of 0.13%, which demonstrated that small changes on the phosphorus center can impact device performance. Encouragingly, PPF-BDTT-S showed a relatively high V_{oc} of 0.90 V and a better PCE than PPF-BDTT. Although the exact reason for the improved performance is

Fig. 3. Comparison of PPF-BDTT, PPF-BDTT-S, and PPF-BDTT-Au ^{31}P NMR spectra (202.5 MHz, 298 K, $CDCl_3$).
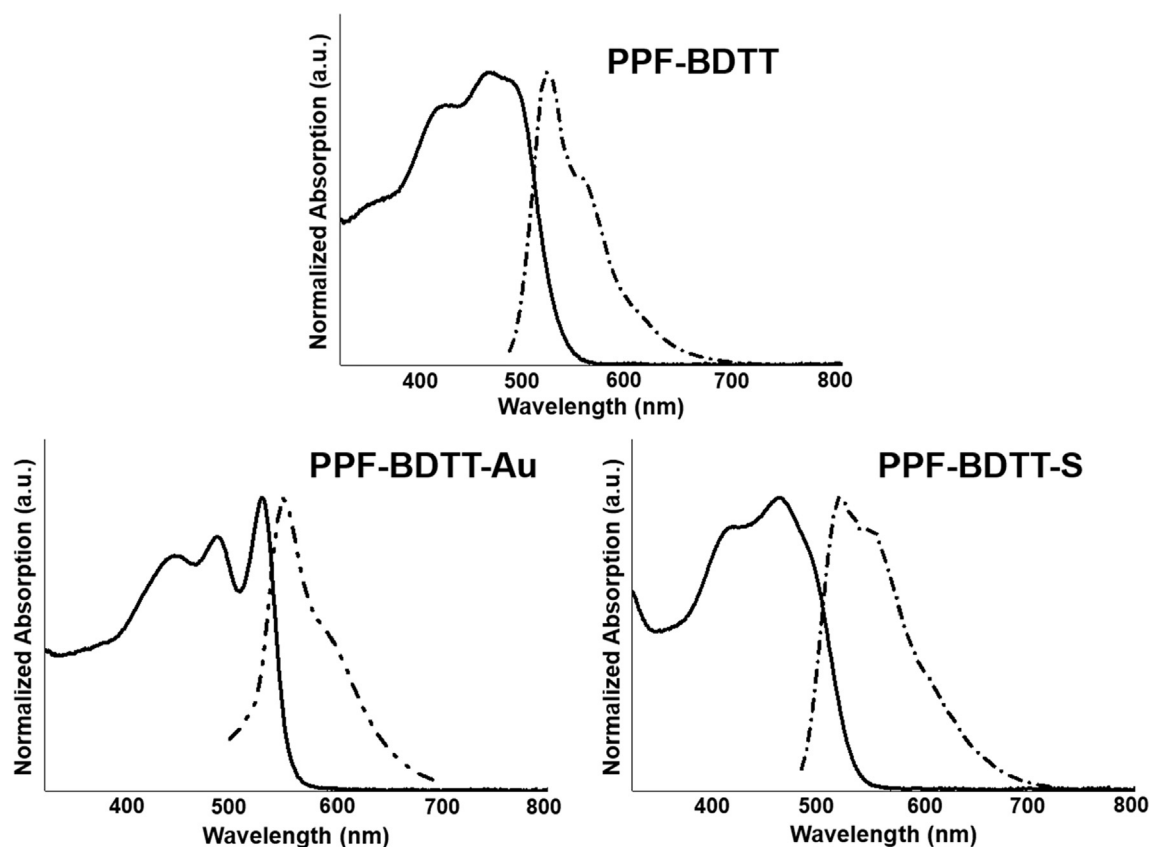
Fig. 4. Normalized UV-vis absorption spectra (solid lines) and emission spectra (dashed lines) of PPF-BDTT, PPF-BDTT-Au and PPF-BDTT-S measured in DCM.

not immediately clear, similar substitutions of sulfur atoms for oxygen atoms in conjugated dimides was observed to improve charge mobility in OFETS [67,68].

In comparison, a solar cell based on the structurally related PDTP-BDTT (DTP = dithienophosphole oxide), was reported to have a PCE of 5.98% [49], which is much higher than that of PPF-BDTT (0.13%). Many factors could contribute to the poor performance of PPF-BDTT compared to PDTP-BDTT. For example, PPF-BDTT has a lower molecular weight of 11.0 kDa (22.0 kDa for PDTP-BDTT); usually polymers with higher molecular weight show better device performance [73,74]. In addition, the wide optical band gap of PPF-BDTT results in absorption to 538 nm and poor utilization of the solar spectrum, while PDTP-BDTT has a narrower optical band gap and absorbs out to 656 nm [49].

4. Conclusion

A new polymerizable phosphafluorene and its copolymer with benzodithiophene PPF-BDTT were synthesized and studied. Post-polymerization modification of PPF-BDTT using easily accessible methods

such as reduction, thiolation, and metal coordination produced the phosphine sulfide polymer PPF-BDTT-S and phosphine gold chloride polymer PPF-BDTT-Au, which demonstrated a powerful and efficient pathway to functionalize organophosphorus polymers.

The optical and electrochemical properties of these polymers were studied, showing the effect of different substituents on the phosphorus atom on the properties of the polymers. The absorption spectra of PPF-BDTT and PPF-BDTT-S are very similar, while PPF-BDTT-Au showed a unique triple peak absorption pattern with a redshift of 65 nm. Compared with other BDTT containing copolymers with different electron-acceptor moieties, these PPF-BDTT and its derivative polymers show higher energy levels and wider bandgaps. To further explore the applications of these polymers, solar cell devices comprising of PPF-BDTT, PPF-BDTT-S, and PPF-BDTT-Au were fabricated, and average PCEs of 0.13%, 0.60%, and 0.26% were obtained, respectively. Despite the relatively low performance, we demonstrated that small changes on phosphorus could affect materials properties and examined, for the first time, the potential abilities of phosphafluorene based polymers as electron donors for application in organic solar cells.

Table 1
Photophysical and Electrochemical Data.

Compound	λ_{ab}[a] (nm)	λ_{em}[a] (nm)	$\log\varepsilon$	λ_{onset} (nm)	LUMO[b] (eV)	HOMO[b] (eV)	$E_{g,cv}$[b] (eV)
PPF-BDTT	465	521	4.38	538	−2.99	−5.56	2.57
PPF-BDTT-S	466	520	4.57	534	−3.03	−5.46	2.43
PPF-BDTT-Au	530	550	4.55	555	−3.43	−5.23	1.80

[a] In DCM (10^{-5} M).

[b] Polymers were measured by casting a film on a working electrode in a 0.1 M solution of Bu_4NClO_4 in acetonitrile at a scan rate of $0.1\,V\,s^{-1}$, E_{ox} (E_{red}) estimated from oxidation(reduction) onset potentials vs ferrocene/ferrocenium, HOMO/LUMO $= -(E_{ox}/E_{red} + 5.1\,eV)$.
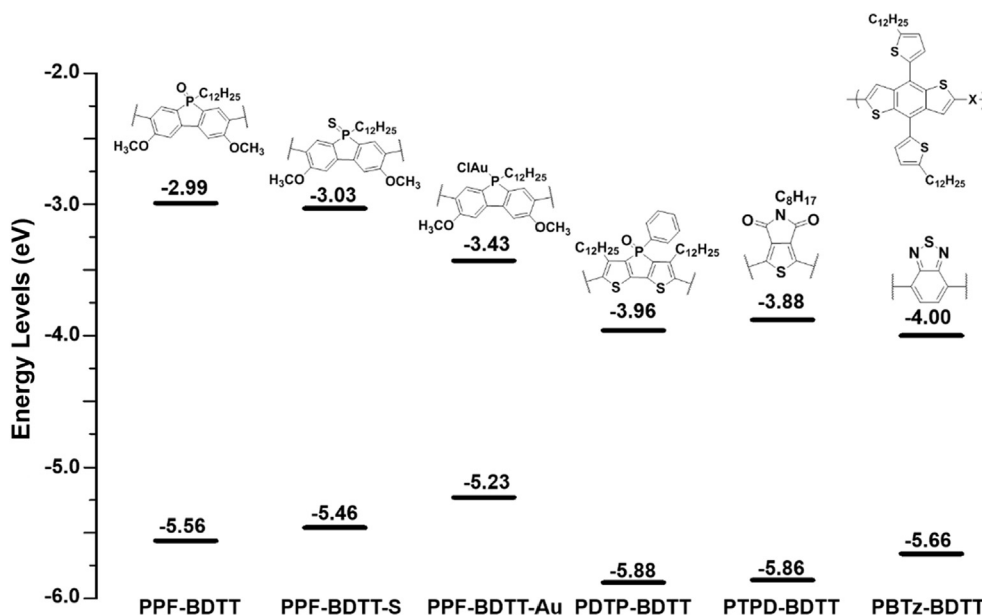
Fig. 5. Energy gap diagram of BDTT-containing copolymers with various electron acceptors. All HOMO and LUMO values were measured or recalculated using the equation LUMO/HOMO $= -(E_{red}/E_{ox} + 5.1 \text{ eV})$ [70].

Appendix A. Supplementary material

Supplementary data associated with this article can be found, in the online version, at https://doi.org/10.1016/j.eurpolymj.2018.05.009.

References

[1] Z. Zheng, S. Zhang, J. Zhang, Y. Qin, W. Li, R. Yu, Z. Wei, J. Hou, Over 11% efficiency in tandem polymer solar cells featured by a low-band-gap polymer with fine-tuned properties, Adv. Mater. 28 (2016) 5133–5138.

[2] L. Dou, Y. Liu, Z. Hong, G. Li, Y. Yang, Low-bandgap near-IR conjugated polymers/molecules for organic electronics, Chem. Rev. 115 (2015) 12633–12665.

[3] L. Lu, T. Zheng, Q. Wu, A.M. Schneider, D. Zhao, L. Yu, Recent advances in bulk heterojunction polymer solar cells, Chem. Rev. 115 (2015) 12666–12731.

[4] X. Xu, K. Feng, K. Li, Q. Peng, Synthesis and photovoltaic properties of two-dimensional benzodithiophene-thiophene copolymers with pendent rational naphtho[1,2-c:5,6-c]bis[1,2,5]thiadiazole side chains, J. Mater. Chem. A 3 (2015) 23149–23161.

[5] B. Kan, H. Feng, X. Wan, F. Liu, X. Ke, Y. Wang, Y. Wang, H. Zhang, C. Li, J. Hou, Y. Chen, Small-molecule acceptor based on the heptacyclic benzodi(cyclopenta-dithiophene) unit for highly efficient nonfullerene organic solar cells, J. Am. Chem. Soc. 139 (2017) 4929–4934.

[6] X. Xu, Z. Li, Z. Wang, K. Li, K. Feng, Q. Peng, 10.20% Efficiency polymer solar cells via employing bilaterally hole-cascade diazaphenanthrobisthiadiazole polymer donors and electron-cascade indene-C70 bisadduct acceptor, Nano Energy 25 (2016) 170–183.

[7] C. Kanimozhi, N. Yaacobi-Gross, K.W. Chou, A. Amassian, T.D. Anthopoulos, S. Patil, Diketopyrrolopyrrole–diketopyrrolopyrrole-based conjugated copolymer for high-mobility organic field-effect transistors, J. Am. Chem. Soc. 134 (2012) 16532–16535.

[8] J. Mei, H.-C. Wu, Y. Diao, A. Appleton, H. Wang, Y. Zhou, W.-Y. Lee, T. Kurosawa, W.-C. Chen, Z. Bao, Effect of spacer length of siloxane-terminated side chains on charge transport in isoindigo-based polymer semiconductor thin films, Adv. Func. Mater. 25 (2015) 3455–3462.

[9] Y.-Q. Zheng, T. Lei, J.-H. Dou, X. Xia, J.-Y. Wang, C.-J. Liu, J. Pei, Strong electron-deficient polymers lead to high electron mobility in air and their morphology-dependent transport behaviors, Adv. Mater. 28 (2016) 7213–7219.

[10] C. Wang, H. Dong, W. Hu, Y. Liu, D. Zhu, Semiconducting π-conjugated systems in field-effect transistors: a material odyssey of organic electronics, Chem. Rev. 112 (2012) 2208–2267.

[11] M.E. Cinar, T. Ozturk, Thienothiophenes, dithienothiophenes, and thienoacenes: syntheses, oligomers, polymers, and properties, Chem. Rev. 115 (2015) 3036–3140.

[12] A.C. Grimsdale, K. Leok Chan, R.E. Martin, P.G. Jokisz, A.B. Holmes, Synthesis of light-emitting conjugated polymers for applications in electroluminescent devices, Chem. Rev. 109 (2009) 897–1091.

[13] S. Rochat, T.M. Swager, Conjugated amplifying polymers for optical sensing applications, ACS Appl. Mater. Interfaces 5 (2013) 4488–4502.

[14] B. Koo, T.M. Swager, Interfacial pressure/area sensing: dual-fluorescence of amphiphilic conjugated polymers at water interfaces, ACS Macro Lett. 6 (2017) 134–138.

[15] J.G. Weis, T.M. Swager, Thiophene-fused tropones as chemical warfare agent-responsive building blocks, ACS Macro Lett. 4 (2015) 138–142.

[16] J.-I. Lee, G. Klaerner, R.D. Miller, Oxidative stability and its effect on the photoluminescence of poly(fluorene) derivatives: end group effects, Chem. Mater. 11 (1999) 1083–1088.

[17] S. Setayesh, D. Marsitzky, K. Müllen, Bridging the gap between polyfluorene and ladder-poly-p-phenylene: synthesis and characterization of poly-2,8-indeno-fluorene, Macromolecules 33 (2000) 2016–2020.

[18] F. Huang, H. Wu, D. Wang, W. Yang, Y. Cao, Novel electroluminescent conjugated polyelectrolytes based on polyfluorene, Chem. Mater. 16 (2004) 708–716.

[19] Y.-C. Pao, Y.-L. Chen, Y.-T. Chen, S.-W. Cheng, Y.-Y. Lai, W.-C. Huang, Y.-J. Cheng, Synthesis and molecular properties of tricyclic biselenophene-based derivatives with nitrogen, silicon, germanium, vinylidene, and ethylene bridges, Org. Lett. 16 (2014) 5724–5727.

[20] X. Yin, F. Guo, R.A. Lalancette, F. Jäkle, Luminescent main-chain organoborane polymers: highly robust, electron-deficient poly(oligothiophene borane)s via stille coupling polymerization, Macromolecules 49 (2016) 537–546.

[21] H. Cao, I.A. Brettell-Adams, F. Qu, P.A. Rupar, Bridged difurans: stabilizing furan with p-block elements, Organometallics 36 (2017) 2565–2572.

[22] H. Cao, P.A. Rupar, Recent advances in conjugated furans, Chem. Eur. J. 23 (2017) 14670–14675.

[23] S.-Y. Liou, C.-S. Ke, J.-H. Chen, Y.-W. Luo, S.-Y. Kuo, Y.-H. Chen, C.-C. Fang, C.-Y. Wu, C.-M. Chiang, Y.-H. Chan, Tuning the emission of semiconducting polymer dots from green to near-infrared by alternating donor monomers and their applications for in vivo biological imaging, ACS Macro Lett. 5 (2016) 154–157.

[24] H. Usta, G. Lu, A. Facchetti, T.J. Marks, Dithienosilole− and dibenzosilole−thiophene copolymers as semiconductors for organic thin-film transistors, J. Am. Chem. Soc. 128 (2006) 9034–9035.

[25] F. Lombeck, H. Komber, D. Fazzi, D. Nava, J. Kuhlmann, D. Stegerer, K. Strassel, J. Brandt, A.D. de Zerio Mendaza, C. Müller, W. Thiel, M. Caironi, R. Friend, M. Sommer, On the effect of prevalent carbazole homocoupling defects on the photovoltaic performance of PCDTBT:PC71BM solar cells, Adv. Energy Mater. 6 (2016) 1601232.

[26] M. Wakioka, M. Ishiki, F. Ozawa, Synthesis of donor-acceptor polymers containing thiazolo[5,4-d]thiazole units via palladium-catalyzed direct arylation polymerization, Macromolecules 48 (2015) 8382–8388.

[27] Y. Yabusaki, N. Ohshima, H. Kondo, T. Kusamoto, Y. Yamanoi, H. Nishihara, Versatile synthesis of blue luminescent siloles and germoles and hydrogen-bond-assisted color alteration, Chem. Eur. J. 16 (2010) 5581–5585.

[28] N. Allard, R.B. Aïch, D. Gendron, P.-L.T. Boudreault, C. Tessier, S. Alem, S.-C. Tse, Y. Tao, M. Leclerc, Germafluorenes: new heterocycles for plastic electronics, Macromolecules 43 (2010) 2328–2333.

[29] V.H.K. Fell, A. Mikosch, A.-K. Steppert, W. Ogieglo, E. Senol, D. Canneson, M. Bayer, F. Schoenebeck, A. Greilich, A.J.C. Kuehne, Synthesis and optical characterization of hybrid organic-inorganic heterofluorene polymers, Macromolecules 50 (2017) 2338–2343.

[30] J. Li, A.C. Grimsdale, Carbazole-based polymers for organic photovoltaic devices,

Chem. Soc. Rev. 39 (2010) 2399–2410.

[31] M.F. Smith, S.J. Cassidy, I.A. Adams, M. Vasiliu, D.L. Gerlach, D.A. Dixon, P.A. Rupar, Substituent effects on the properties of borafluorenes, Organometallics 35 (2016) 3182–3191.

[32] C. Dou, X. Long, Z. Ding, Z. Xie, J. Liu, L. Wang, An electron-deficient building block based on the B←N unit: an electron acceptor for all-polymer solar cells, Angew. Chem., Int. Ed. 55 (2016) 1436–1440.

[33] S. Saito, K. Matsuo, S. Yamaguchi, Polycyclic π-electron system with boron at its center, J. Am. Chem. Soc. 134 (2012) 9130–9133.

[34] C. Dou, S. Saito, K. Matsuo, I. Hisaki, S. Yamaguchi, A Boron-Containing, PAH as a substructure of boron-doped graphene, Angew. Chem., Int. Ed. 51 (2012) 12206–12210.

[35] I.A. Adams, P.A. Rupar, A poly(9-borafluorene) homopolymer: an electron-deficient polyfluorene with "turn-on" fluorescence sensing of NH3 vapor, Macromol. Rapid Commun. 36 (2015) 1336–1340.

[36] T. Matsumoto, K. Tanaka, Y. Chujo, Synthesis and characterization of gallafluorene-containing conjugated polymers: control of emission colors and electronic effects of gallafluorene units on π-conjugation system, Macromolecules 48 (2015) 1343–1351.

[37] T. Matsumoto, K. Tanaka, Y. Chujo, Synthesis and optical properties of stable gallafluorene derivatives: investigation of their emission via triplet states, J. Am. Chem. Soc. 135 (2013) 4211–4214.

[38] T. Baumgartner, Insights on the design and electron-acceptor properties of conjugated organophosphorus materials, Acc. Chem. Res. 47 (2014) 1613–1622.

[39] C. Reus, T. Baumgartner, Stimuli-responsive chromism in organophosphorus chemistry, Dalton Trans. 45 (2016) 1850–1855.

[40] C. Reus, M. Stolar, J. Vanderkley, J. Nebauer, T. Baumgartner, A convenient N-arylation route for electron-deficient pyridines: the case of π-extended electro-chromic phosphaviologens, J. Am. Chem. Soc. 137 (2015) 11710–11717.

[41] X. He, J.-B. Lin, W.H. Kan, T. Baumgartner, Phosphinine lipids: a successful marriage between electron-acceptor and self-assembly features, Angew. Chem., Int. Ed. 52 (2013) 8990–8994.

[42] X. He, J.-B. Lin, W.H. Kan, P. Dong, S. Trudel, T. Baumgartner, Molecular engineering of "click"-pholes towards self-assembled luminescent soft materials, Adv. Funct. Mater. 24 (2014) 897–906.

[43] Y. Dienes, M. Eggenstein, T. Neumann, U. Englert, T. Baumgartner, Synthesis and optoelectronic properties of transition metal complexes incorporating dithieno[3,2-b:2[prime or minute],3[prime or minute]-d]phosphole ligands, Dalton Trans. 1424–1433 (2006).

[44] X. He, J. Borau-Garcia, A.Y.Y. Woo, S. Trudel, T. Baumgartner, Dithieno[3,2-c:2′,3′-e]-2,7-diketophosphepin: a unique building block for multifunctional π-conjugated materials, J. Am. Chem. Soc. 135 (2013) 1137–1147.

[45] C. Fave, T.-Y. Cho, M. Hissler, C.-W. Chen, T.-Y. Luh, C.-C. Wu, R. Réau, First examples of organophosphorus-containing materials for light-emitting diodes, J. Am. Chem. Soc. 125 (2003) 9254–9255.

[46] H.-C. Su, O. Fadhel, C.-J. Yang, T.-Y. Cho, C. Fave, M. Hissler, C.-C. Wu, R. Réau, Toward functional π-conjugated organophosphorus materials: design of phosphole-based oligomers for electroluminescent devices, J. Am. Chem. Soc. 128 (2006) 983–995.

[47] B.W. Rawe, M.R. Scott, C.M. Brown, H.K. MacKenzie, D.P. Gates, Poly(p-phenylenediethynylene phosphine)s and related π-conjugated phosphine-diyne polymers: synthesis, Characterization Photophysical Prop. Macromol. 50 (2017) 8916–8927.

[48] M. Sebastian, M. Hissler, C. Fave, J. Rault-Berthelot, C. Odin, R. Réau, Phosphole-modified poly(thiophene)s: unique postfunctionalizable conjugated polymers that sense elemental chalcogenides, Angew. Chem., Int. Ed. 45 (2006) 6152–6155.

[49] K.H. Park, Y.J. Kim, G.B. Lee, T.K. An, C.E. Park, S.-K. Kwon, Y.-H. Kim, Recently advanced polymer materials containing dithieno[3,2-b:2′,3′-d]phosphole oxide for efficient charge transfer in high-performance solar cells, Adv. Funct. Mater. 25 (2015) 3991–3997.

[50] Y.J. Kim, M.J. Kim, T.K. An, Y.H. Kim, C.E. Park, A new multi-functional conjugated polymer for use in high-performance bulk heterojunction solar cells, Chem. Commun. 51 (2015) 11572–11575.

[51] R.-F. Chen, R. Zhu, Q.-L. Fan, W. Huang, Synthesis, structure, and optoelectronic properties of phosphafluorene copolymers, Org. Lett. 10 (2008) 2913–2916.

[52] S. Zhang, R. Chen, J. Yin, F. Liu, H. Jiang, N. Shi, Z. An, C. Ma, B. Liu, W. Huang, Tuning the optoelectronic properties of 4,4′-N, N′-dicarbazole-biphenyl through

heteroatom linkage: new host materials for phosphorescent organic light-emitting diodes, Org. Lett. 12 (2010) 3438–3441.

[53] X. Xu, H. Guo, J. Zhao, B. Liu, X. Yang, G. Zhou, Z. Wu, Asymmetric tris-heteroleptic iridium[iii] complexes containing a 9-phenyl-9-phosphafluorene oxide moiety with enhanced charge carrier injection/transporting properties for highly efficient solution-processed organic light-emitting diodes, Chem. Mater. 28 (2016) 8556–8569.

[54] R. Kabe, V.M. Lynch, P. Anzenbacher Jr, Enhanced phosphorescence in dibenzo-phosphole chalcogenide mixed crystal, CrystEngComm 13 (2011) 5423–5427.

[55] R.-F. Chen, Q.-L. Fan, C. Zheng, W. Huang, A general strategy for the facile synthesis of 2,7-dibromo-9-heterofluorenes, Org. Lett. 8 (2006) 203–205.

[56] Y. Kuninobu, T. Yoshida, K. Takai, Palladium-catalyzed synthesis of dibenzo-phosphole oxides via intramolecular dehydrogenative cyclization, J. Org. Chem. 76 (2011) 7370–7376.

[57] K. Baba, M. Tobisu, N. Chatani, Palladium-catalyzed direct synthesis of phosphole derivatives from triarylphosphines through cleavage of carbon-hydrogen and carbon-phosphorus bonds, Angew. Chem., Int. Ed. 52 (2013) 11892–11895.

[58] M. Yoshikazu, T. Teruyuki, T. Masato, Poly[2,7-(9-oxo-9-phosphafluorenylene)-alt-co-(1,4-arylene)]s: phosphorus-containing π-conjugated polymers, Chem. Lett. 33 (2004) 44–45.

[59] H. Benten, D. Mori, H. Ohkita, S. Ito, Recent research progress of polymer donor/polymer acceptor blend solar cells, J. Mater. Chem. A 4 (2016) 5340–5365.

[60] Z.-G. Zhang, J. Wang, Structures and properties of conjugated Donor-Acceptor co-polymers for solar cell applications, J. Mater. Chem. 22 (2012) 4178–4187.

[61] R.S. Kularatne, H.D. Magurudeniya, P. Sista, M.C. Biewer, M.C. Stefan, Donor–acceptor semiconducting polymers for organic solar cells, J. Polym. Sci. A Polym. Chem. 51 (2013) 743–768.

[62] K. Müllen, W. Pisula, Donor-acceptor polymers, J. Am. Chem. Soc. 137 (2015) 9503–9505.

[63] J. Yuan, Z. Zhai, H. Dong, J. Li, Z. Jiang, Y. Li, W. Ma, Efficient polymer solar cells with a high open circuit voltage of 1 V, Adv. Func. Mater. 23 (2013) 885–892.

[64] R.S. Rogers, A general synthesis of phosphonic acid dichlorides using oxalyl chloride and DMF catalysis, Tetrahedron Lett. 33 (1992) 7473–7474.

[65] H. Yao, L. Ye, H. Zhang, S. Li, S. Zhang, J. Hou, Molecular design of benzodithio-phene-based organic photovoltaic materials, Chem. Rev. 116 (2016) 7397–7457.

[66] L. Ye, S. Zhang, L. Huo, M. Zhang, J. Hou, Molecular design toward highly efficient photovoltaic polymers based on two-dimensional conjugated benzodithiophene, Acc. Chem. Res. 47 (2014) 1595–1603.

[67] T.-F. Yang, S.-H. Huang, Y.-P. Chiu, B.-H. Chen, Y.-W. Shih, Y.-C. Chang, J.-Y. Yao, Y.-J. Lee, M.-Y. Kuo, Pyromellitic dithioimides: thionation improves air-stability and electron mobility of N-type organic field-effect transistors, Chem. Commun. 51 (2015) 13772–13775.

[68] L.M. Kozycz, C. Guo, J.G. Manion, A.J. Tilley, A.J. Lough, Y. Li, D.S. Seferos, Enhanced electron mobility in crystalline thionated naphthalene diimides, J. Mater. Chem. C 3 (2015) 11505–11515.

[69] H. Chen, W. Delaunay, J. Li, Z. Wang, P.-A. Bouit, D. Tondelier, B. Geffroy, F. Mathey, Z. Duan, R. Réau, M. Hissler, Benzofuran-fused phosphole: synthesis, electronic, and electroluminescence properties, Org. Lett. 15 (2013) 330–333.

[70] C.M. Cardona, W. Li, A.E. Kaifer, D. Stockdale, G.C. Bazan, Electrochemical considerations for determining absolute frontier orbital energy levels of conjugated polymers for solar cell applications, Adv. Mater. 23 (2011) 2367–2371.

[71] P. Sista, R.S. Kularatne, M.E. Mulholland, M. Wilson, N. Holmes, X. Zhou, P.C. Dastoor, W. Belcher, S.C. Rasmussen, M.C. Biewer, M.C. Stefan, Synthesis and photovoltaic performance of donor–acceptor polymers containing benzo[1,2-b:4,5-b′]dithiophene with thienyl substituents, J. Polym. Sci. A Polym. Chem. 51 (2013) 2622–2630.

[72] S.A. Elkassih, P. Sista, H.D. Magurudeniya, A. Papadimitratos, A.A. Zakhidov, M.C. Biewer, M.C. Stefan, Phenothiazine semiconducting polymer for light-emitting diodes, Macromol. Chem. Phys. 214 (2013) 572–577.

[73] C. Ta-Ya, L. Jianping, B. Serge, Z. Yanguang, P. Jean-Rémi, Z. Jiayun, N. Ahmed, L. Mario, T. Ye, Effects of the molecular weight and the side-chain length on the photovoltaic performance of dithienosilole/thienopyrrolodione copolymers, Adv. Func. Mater. 22 (2012) 2345–2351.

[74] C. Liu, K. Wang, X. Hu, Y. Yang, C.-H. Hsu, W. Zhang, S. Xiao, X. Gong, Y. Cao, Molecular weight effect on the efficiency of polymer solar cells, ACS Appl. Mater. Interfaces 5 (2013) 12163–12167.